*Neuropathology and Applied Neurobiology* (2014), **40**, 345–350 doi: 10.1111/nan.12058

# Scientific correspondence

## Cerebrotendinous xanthomatosis with the c.379C>T (p.R127W) mutation in the *CYP27A1* gene associated with premature age-associated limbic tauopathy

Cerebrotendinous xanthomatosis (CTX) is an autosomal recessive disease associated with mutations in the mitochondrial *CYP27A1* gene [1]. The deficiency of sterol 27-hydroxylase leads to the disturbance of bile acid synthesis and causes a multisystem disorder, including signs of premature ageing like cataracts or atherosclerosis. In addition, neuropsychiatric symptoms, like dementia, cerebellar ataxia, pyramidal signs, seizures or extrapyramidal symptoms may occur [1]. Magnetic resonance imaging (MRI) examinations emphasize cerebellar atrophy and bilateral lesions in the cerebellar white matter, while occasional neuropathological studies described granulomatous and xanthomatous changes mainly in the cerebellar hemispheres, globus pallidus and cerebellar peduncles [1]. There is a paucity of information whether age-related neurodegenerative diseases are present in CTX or not. We report the clinical, biochemical and neuropathological features of CTX associated with neuron-predominant tau pathology predominating in the limbic system, which was compatible with age-dependent argyrophilic grain disease.

Two Hungarian adult siblings were examined. The elder brother died at the age of 46, and his brother is still alive at the age of 43 and presented with a similar clinical course (summarized in Table 1). The analyses presented here were performed as diagnostic tests and consent for publication was obtained from their mother. In both patients mitochondrial encephalopathy was suspected clinically. During the childhood of patient 1, diarrhoea and anaemia was reported. At elementary school a psychological examination showed moderate mental deficiency. At the age of 14 his IQ was 73. Ten years later hepatomegaly was noted. Two years later cataract was diagnosed in both eyes. Furthermore, due to cognitive impairment and aggression he left his job as an unskilled worker. Soon gait disorder and ataxia evolved and progressed to a spastico-paretico-ataxic gait, together with dysarthria, tetrapyramidal symptoms and tetraparesis. At the age of 45 he had epileptic seizures, his state deteriorated and he died due to bronchopneumonia.

General autopsy showed severe atherosclerosis, fibrotic degeneration of myocardium and fatty degeneration of the liver. Neuropathological studies were performed as described using a panel of antibodies against neurodegeneration-related proteins [2], including amyloid-beta (A-beta; 1:50, clone 6F/3D, Dako, Glostrup, Denmark), alpha-synuclein (clone 5G4, 1:2000, Roboscreen, Leipzig, Germany), phospho-TDP-43 (pS409/410, 1:2000, Cosmo Bio, Tokyo, Japan), anti-p62 (1:500, BD Biosciences, San Jose, CA, USA), anti-ubiquitin (1:50 000, Millipore, Temecula, CA, USA), and a panel of anti-tau antibodies: anti-tau AT8 (pS202, 1:200), AT100 (pS212, 1:200), AT180 (pT231, 1:200), AT270 (pT181, 1:200), HT7 (tau 169-163, 1:100; all from Pierce Biotechnology, Rockford, IL, USA), anti-4R tau (RD4, 1:200, Upstate, Charlottesville, VA, USA), anti-3R tau (RD3, 1:2000, Upstate). The DAKO EnVision© detection kit, peroxidase/DAB, rabbit/mouse (Dako) was used for visualization of antibody reactions. In addition, Haematoxylin and Eosin, Luxol Fast Blue/nuclear fast red, periodic acid-Schiff (PAS), Sudan-black, and Bielschowsky and Gallyas silver stainings were performed.

Four major alterations were observed: (1) xanthomatous changes; (2) loss of axons and myelin in the white matter; (3) neuronal loss and reactive astrogliosis; and (4) limbic tauopathy compatible with argyrophilic grain disease. Accumulation of perivascular macrophages, multinucleated giant cells, fibrotic vessels and cholesterol clefts (Figure 1**A–D**) predominated in the cerebellar white matter, dentate nucleus, globus pallidus, cerebral peduncles, pontine base, and pyramids (Table 2). PAS positive granular material accumulated in the perivascular space; ultrastructurally these were composed of convolutes of membranes that were about 12–15 nm thick (Figure 1**E,F**). In addition these showed autofluorescence and were Sudan black positive indicative of lipids (online Figure S1). Prominent loss of myelin and axons (Figure 1**G**), and PAS-positive degradation products in macrophages together with perivascular CD8-positive T cells (Figure 1**H**) were seen mainly in the cerebellum, cerebral peduncles, pontine base (transverse fibres preserved) and pyramids. Neuronal loss was prominent in the inferior olives, dentate nucleus and cerebellar cortex associated with reactive microgliosis (Figure 1**I**). Reactive astrogliosis

**Table 1.** Summary of clinical data

| | *Patient 1* | *Patient 2* |
|---|---|---|
| Age | 46 years at death | 43 years at the last examination |
| Sex | Male | Male |
| Genetic examination | – | + |
| Neuropathological examination | + | – |
| MRI | – | + |
| Childhood diarrhoea | + | + |
| Juvenile cataracts | + | + |
| Tendon xanthomas | + | + |
| Hepatomegaly | + | + |
| Osteoporosis | – | + |
| Early neurological symptoms | | |
| Cognitive impairment | + | + |
| Gait disorder | + | – |
| Ataxia | + | – |
| Symptoms during the course | | |
| Dysarthria | + | + |
| Pyramidal signs | + | + |
| Spastic tetraparesis | + | + |
| Dysphagia | + | – |
| Peripheral neuropathy | – | + |
| Mental deterioration | + | + |
| Aggressivity | + | + |
| Epileptic seizures | + | – |

was seen in the amygdala (Figure 1**J**). There was a lack of neuritic plaques in silver staining, as well as a complete lack of A-beta immunoreactive parenchymal or vascular deposits, phospho-TDP-43 or alpha-synuclein immunoreactive pathological structures; however, immunostaining for phospho-tau (AT8, pS202) revealed widespread alterations. Tau pathology predominated in the limbic system (Table 2 and Figure S1), in particular the amygdala and hippocampus CA1 subregion (Figure 1**K**,**L**). It was characterized by diffuse neuronal cytoplasmic labelling, grains, fine granular immunoreactivity in the astrocytic processes, and oligodendroglial coiled bodies in the amygdala and hippocampus white matter (Figure 1**M**). Neuronal tau immunoreactivity and fine threads were observed in cortical areas as well as in the locus ceruleus (Figure 1**N**). Tau pathology was mostly seen using anti-tau AT8 (pS202) AT100 (pS212), AT180 (pT231), but was significantly less using AT270 (pT181) and HT7 (tau 169-163) antibodies. All these structures were nearly exclusively immunoreactive for the 4R tau isoform (Figure 1**O**), while only the neurofibrillary tangles were immunopositive for the 3R isoform. Grains and scattered tangles were immunoreactive for ubiquitin and p62 (Figure 1**P**) and were argyrophilic using the Gallyas silver stain. The dentate gyrus did not show p62/ubiquitin or phospho-TDP-43 immunoreactive structures.

The first complaint of patient 2 was diarrhoea at 4 months of age. He had learning difficulties at school. Cataracts were diagnosed at 25 years of age. Due to hyperbilirubinaemia and hepatomegaly Gilbert disease was suspected. The first neurological examination was performed due to pain in his lower limbs. Positive Babinski sign was found on the right side. Soon he experienced gait disorder and muscle weakness. Electroneurography revealed symmetrical decrease in the conduction velocity of the peroneal nerve and electromyography showed signs of a neurogenic lesion, confirmed also by muscle biopsy. At the age of 35, gait ataxia, hyperreflexia and pyramidal signs were described. His state deteriorated and dysarthria and insomnia was documented. At the age of 42 dementia and tetraparesis were noted. Cranial MRI revealed bilateral high signal intensities in FLAIR and T2 sequences in the cerebellar white matter and brainstem (Figure 1**Q–S**). Plasma cholestanol was determined following the modified method of Ahmida *et al.* [3] using gas chromatography and mass spectrometry. Spectra of sterol derivatives were identified by comparison with those from standards and those reported in the National Institute of Standards and Technology (NIST) library. Exons of the *CYP27A1* gene were amplified by seven PCR reactions. PCR products were examined by bidirectional DNA sequencing. Plasma cholestanol concentration of patient 2 (76.4 μmol/l) was highly above the normal range (2–12.6 μmol/l) and was in the diagnostic range [4]. He was homozygous for the mutation c.379C>T (p.R127W).

The clinical phenotype of our patients is compatible with the spectrum of clinical symptoms associated with CTX and the mutation detected has been also reported [1]. The dystrophic changes affecting the cerebellar white matter seen both in neuropathology and in MRI have been described [1,5]. However, histopathological evidence of age-related neurodegenerative disease has not yet been reported in CTX. Interestingly, we did not observe senile plaques or deposition of A-beta in the parenchyma or cerebral vessels as described in Alzheimer's disease (AD). As an AD-associated morphological feature, neurofibrillary degeneration was compatible with Braak and Braak Stage III with the note that low number of threads and neuronal tau immunoreactivity was seen in neocortical areas and substantia nigra as well [6]. Another mutation associated with CTX showed mild neurofibrillary degeneration

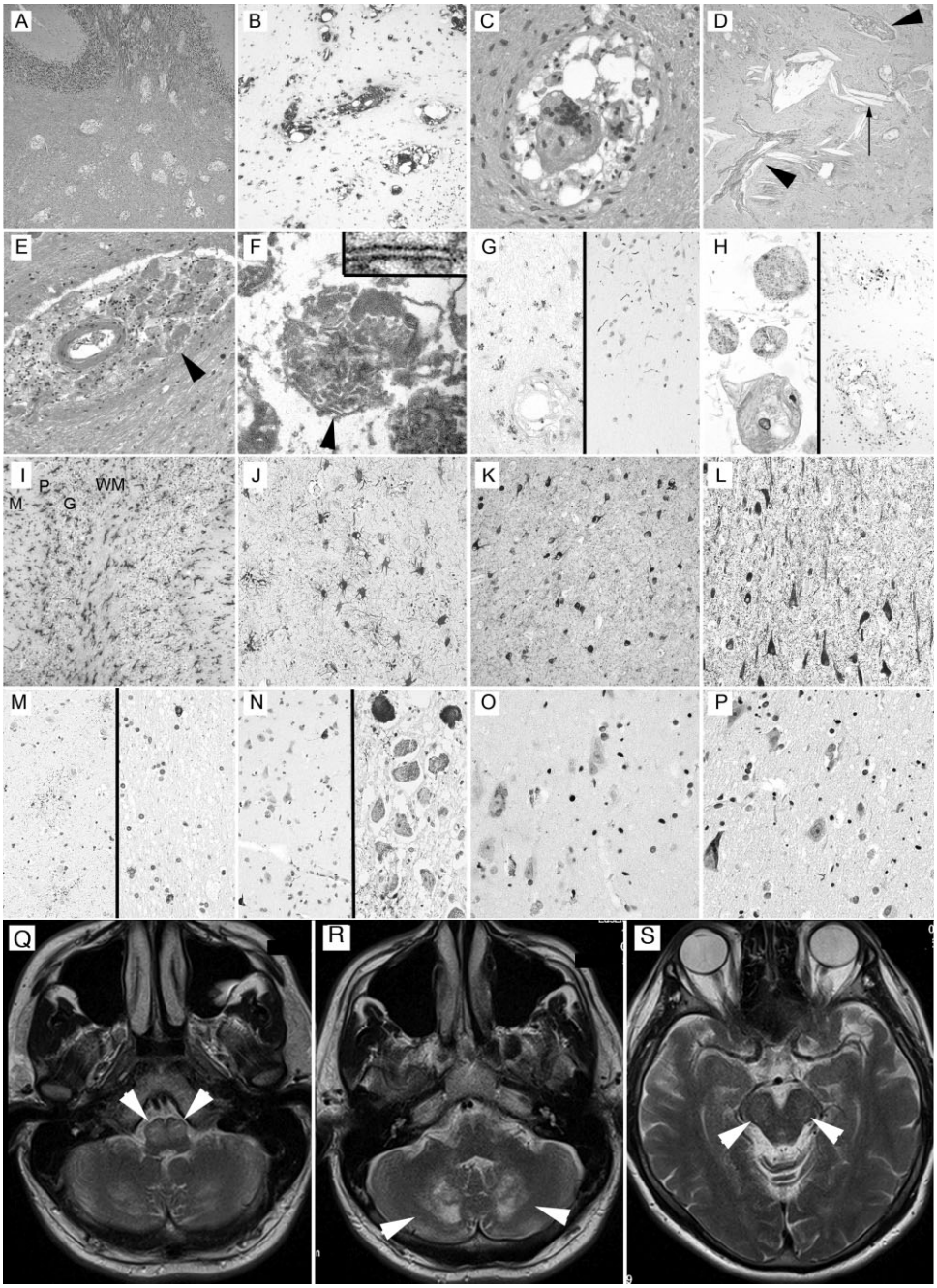


**Figure 1.** Neuropathological alterations (patient 1). Cerebellar white matter (**A**) with CD68 immunoreactive perivascular macrophages (**B**) that are often multinucleated (**C**). Fibrotic vessels (arrowheads) and cholesterol clefts (arrow) (**D**). Macrophages accumulate granular material (**E**; arrowhead) that shows convolutes of membranes in electron microscopy (**F**; arrowhead enlarged in right upper inset). Prominent demyelination (**G**; left image shown by immunostaining for anti-myelin basic protein) accompanied by axonal lost (**G**; right image using anti-SMI-31 neurofilament immunostaining) and PAS-positive degradation products in macrophages (**H**; left) and perivascular CD8 positive T cells (**H**; right) in the cerebellum. Neuronal loss accompanied by reactive microgliosis in the cerebellar cortex (**I**; M: molecular, P: Purkinje, G: granular layers, WM: white matter). Reactive astrogliosis in the amygdala (**J**). Neuronal tau immunoreactivity in the amygdala (**K**) and hippocampus CA1 subregion (**L**; both AT8 anti-tau immunostaining). Fine granular immunoreactivity in the astrocytic processes (**M**; left) and oligodendroglial coiled bodies (**M**; right; both AT8 immunostaining). Neuronal tau immunoreactivity and threads in the temporal cortex (**N**; left) and in the locus coeruleus (**N**; right). Tau pathology is immunoreactive for 4R tau isoform (**O**). Grains and scattered tangles are immunoreactive for p62 (**P**). MRI images (T2; patient 2) showing bilateral high signal intensities (indicated with white arrowheads) in the medullary pyramid (**Q**), cerebellar white matter (**R**) and cerebral peduncles (**S**).

**Table 2.** Summary of the neuropathological observations (patient 1)

| *Anatomical region* | *Leukodystrophy* | *Gliosis* | *PV Macroph* | *Tauopathy* |
|---|---|---|---|---|
| Frontal Cx | – | – | – | + |
| Cingular Cx | – | – | – | + |
| Parietal Cx | – | – | – | – |
| Temporal Cx | – | – | – | + |
| Occipital Cx | – | – | – | + |
| Hippocampus CA1–CA4 | – | – | – | ++ |
| Dentate gyrus | – | – | – | – |
| Entorhinal Cx | – | – | – | +++ |
| Caudate nucleus | – | + | + | + |
| Accumbens nucleus | – | + | + | + |
| Putamen | – | – | – | + |
| Globus pallidus | – | + | ++ | – |
| Thalamus | – | – | – | – |
| Subthalamic nucleus | – | – | – | – |
| Amygdala | – | ++ | – | +++ |
| Substantia nigra | – | + | – | + |
| Dorsal raphe nucleus | – | + | – | + |
| Locus coeruleus | – | + | – | ++ |
| Dorsal vagus nucleus | – | – | – | + |
| Inferior olives | – | ++ | + | – |
| Dentate nucleus | – | +++ | +++ | – |
| Purkinje cell layer (Cbll) | – | +++ | – | – |
| Molecular layer (Cbll) | – | + | + | – |
| Granular layer (Cbll) | – | ++ | + | – |
| Capsula interna | – | – | – | – |
| Periventricular white matter | – | – | – | – |
| Corpus callosum | – | – | – | – |
| Pedunculus cerebri | ++ | ++ | ++ | – |
| Pontine base | +++ | +++ | +++ | – |
| Pyramids | ++ | ++ | ++ | – |
| Cerebellar white matter | +++ | +++ | +++ | – |

PV Macroph, perivascular macrophages.

without amyloid-beta plaques [7]. However, systematic mapping of tau immunoreactivity revealed prominent limbic tau pathology in our case that was characteristic for an advanced argyrophilic grain disease (AGD), which is an age-dependent disorder [8,9]. It could be theorized that excessive cholestanol may replace cholesterol in the plasma membrane that changes membrane fluidity [10], which, together with activation of stress kinases or mitochondrial dysfunction [1], may cause a limbic tauopathy showing AGD-like neurodegeneration [8,11] in certain mutations. The aetiology of AGD is not known. It may be associated with other tauopathies or AD, and most likely it lowers the threshold for cognitive decline. In the present case we did not observe features of other primary tauopathies, only the AGD-like pathology together with moderate neurofibrillary degeneration (Braak and Braak Stage III). Our observations support the notion that in CTX premature ageing of the brain may not manifest with AD pathology [12], as defined by tangles and A-beta immunoreactive plaques, but may be associated with a limbic predominant tauopathy with features of AGD.

## Acknowledgements

This study was supported by the European Commission's 7th Framework Programme grant number 278486, 'DEVELAGE' (G.G.K.), and by the National Development Agency, Hungary; grant numbers TÁMOP-4-2-1/B-03/1/KMR-2010-20001 (M.J.M.), and TÁMOP-4.2.2.A-11/1/KONV-2012-0031 (M.H.). We have no conflict of interest.

## Author contributions

All authors included on the paper fulfil the criteria of authorship because of their substantial contribution to

acquisition, analysis and interpretation of data, and manuscript preparation and approval.

- István Kapás: acquisition, analysis and interpretation of data, drafting the manuscript, final approval;
- Mónika Katkó: analysis and interpretation of genetic and biochemical data, critical revision of manuscript, final approval;
- Mariann Harangi: analysis and interpretation of genetic and biochemical data, drafting and critical revision of manuscript, final approval;
- György Paragh: analysis and interpretation of genetic and biochemical data, critical revision of manuscript, final approval;
- István Balogh: analysis and interpretation of genetic and biochemical data, critical revision of manuscript, final approval;
- Zoltán Kóczi: acquisition and interpretation of pathology, critical revision of manuscript, final approval;
- Günther Regelsberger: analysis and interpretation of data, critical revision of manuscript, final approval;
- Mária Judit Molnár: analysis and interpretation data, critical revision of manuscript, final approval;
- Gabor G. Kovacs: acquisition, analysis and interpretation of data, drafting the manuscript, supervision, final approval.

**I. Kapás*†**
**M. Katkó‡**
**M. Harangi‡**
**G. Paragh‡**
**I. Balogh§**
**Z. Kóczi¶**
**G. Regelsberger****
**M. J. Molnár††**
**G. G. Kovacs*,****

**Neuropathology and Prion Disease Reference Centre, ††Clinical and Research Centre for Molecular Neurology, Semmelweis University, Budapest, †Department of Neurology, ¶Department of Pathology, County Hospital, Vác, ‡Division of Metabolic Diseases, Department of Medicine, §Department of Laboratory Medicine, University of Debrecen, Debrecen, Hungary, and **Institute of Neurology, Medical University of Vienna, Vienna, Austria*

## References

1 Gallus GN, Dotti MT, Federico A. Clinical and molecular diagnosis of cerebrotendinous xanthomatosis with a review of the mutations in the CYP27A1 gene. *Neurol Sci* 2006; **27**: 143–9
2 Kovacs GG, Molnar K, Laszlo L, Ströbel T, Botond G, Honigschnabl S, Reiner-Concin A, Palkovits M, Fischer P, Budka H. A peculiar constellation of tau pathology defines a subset of dementia in the elderly. *Acta Neuropathol (Berl)* 2011; **122**: 205–22
3 Ahmida HS, Bertucci P, Franzo L, Massoud R, Cortese C, Lala A, Federici G. Simultaneous determination of plasmatic phytosterols and cholesterol precursors using gas chromatography-mass spectrometry (GC-MS) with selective ion monitoring (SIM). *J Chromatogr B Analyt Technol Biomed Life Sci* 2006; **842**: 43–7
4 Pilo de la Fuente B, Sobrido MJ, Giros M, Pozo L, Lustres M, Barrero F, Macarron J, Diaz M, Jimenez-Escrig A. [Usefulness of cholestanol levels in the diagnosis and follow-up of patients with cerebrotendinous xanthomatosis]. *Neurologia* 2011; **26**: 397–404
5 Soffer D, Benharroch D, Berginer V. The neuropathology of cerebrotendinous xanthomatosis revisited: a case report and review of the literature. *Acta Neuropathol (Berl)* 1995; **90**: 213–20
6 Alafuzoff I, Arzberger T, Al-Sarraj S, Bodi I, Bogdanovic N, Braak H, Bugiani O, Del-Tredici K, Ferrer I, Gelpi E, Giaccone G, Graeber MB, Ince P, Kamphorst W, King A, Korkolopoulou P, Kovacs GG, Larionov S, Meyronet D, Monoranu C, Parchi P, Patsouris E, Roggendorf W, Seilhean D, Tagliavini F, Stadelmann C, Streichenberger N, Thal DR, Wharton SB, Kretzschmar H. Staging of neurofibrillary pathology in Alzheimer's disease: a study of the BrainNet Europe Consortium. *Brain Pathol* 2008; **18**: 484–96
7 Wallon D, Guyant-Marechal L, Laquerriere A, Wevers RA, Martinaud O, Kluijtmans LA, Yntema HG, Saugier-Veber P, Hannequin D. Clinical imaging and neuropathological correlations in an unusual case of cerebrotendinous xanthomatosis. *Clin Neuropathol* 2010; **29**: 361–4
8 Ferrer I, Santpere G, van Leeuwen FW. Argyrophilic grain disease. *Brain* 2008; **131**: 1416–32
9 Tolnay M, Clavaguera F. Argyrophilic grain disease: a late-onset dementia with distinctive features among tauopathies. *Neuropathology* 2004; **24**: 269–83
10 Seyama Y. Cholestanol metabolism, molecular pathology, and nutritional implications. *J Med Food* 2003; **6**: 217–24
11 Ilieva EV, Kichev A, Naudi A, Ferrer I, Pamplona R, Portero-Otin M. Mitochondrial dysfunction and oxidative and endoplasmic reticulum stress in argyrophilic grain disease. *J Neuropathol Exp Neurol* 2011; **70**: 253–63
12 Nelson PT, Head E, Schmitt FA, Davis PR, Neltner JH, Jicha GA, Abner EL, Smith CD, Van Eldik LJ, Kryscio RJ, Scheff SW. Alzheimer's disease is not 'brain aging': neuropathological, genetic, and epidemiological human studies. *Acta Neuropathol (Berl)* 2011; **121**: 571–87

## Supporting information

Additional Supporting Information may be found in the online version of this article at the publisher's web-site:

**Figure S1.** Overview of neuropathological alterations. Upper panel: Staining properties of the granular material accumulating in the perivascular space: they are visible in Sudan Black staining (left) and less in Luxol staining (middle image), and they show autofluorescence (right image). Scale bar in the left image represents 0.03 mm. Lower panel: Overview of the tau pathology in the limbic system using immunohistochemistry for AT8 and for RD4. Upper three images represent tau pathology in the amygdala seen at different magnifications (scale bar in the left image represents 2 mm, 0.6 mm and 0.1 mm, from left to right respectively). Middle three images represent tau pathology in the ambient gyrus and hippocampus (scale bar in the left image represents 0.4 mm, 0.6 mm and 0.2 mm, from left to right respectively). Lower three images represent RD4 pathology in the amygdala and entorhinal cortex (scale bar in the left image represents 0.15 mm, 0.15 mm and 0.03 mm, from left to right respectively).

*Received 16 December 2012*
*Accepted after revision 30 April 2013*
*Published online Article Accepted on 10 May 2013*